Macromolecules

ARTICLE

pubs.acs.org/Macromolecules

Combined Synthesis, TGIC Characterization, and Rheological Measurement and Prediction of Symmetric H Polybutadienes and Their Blends with Linear and Star-Shaped Polybutadienes

Xue Chen,[†] M. Shahinur Rahman,[‡] Hyojoon Lee,[§] Jimmy Mays,[‡] Taihyun Chang,[§] and Ronald Larson*[,†]

[†]Department of Chemical Engineering, University of Michigan, Ann Arbor, Michigan 48109, United States

[‡]Department of Chemistry, University of Tennessee, Knoxville, Tennessee 37966, United States

[§] Department of Chemistry and Division of Advanced Materials Science, Pohang University of Science and Technology (POSTECH), Pohang 790-784, Korea

ABSTRACT: We report the synthesis and characterization by temperature gradient interaction chromatography (TGIC) and rheometry of a symmetric H-shaped polybutadiene (PBd) that we call "HA20B40", and of a symmetric star-shaped synthetic precursor of HA20B40, and the use of these characterization data to test and validate advanced tube models (the hierarchical and, to a lesser extent, the BOB models) for long-chain branched polymers. Furthermore, by deliberately adding additional well-characterized linear and star-branched polymers into HA20B40, we mimic the effect of impurities in the sample to test the ability of the hierarchical model to account for the effect of similar such impurities, which are detected by TGIC. Our modeling predictions for HA20B40 and its blends with star and linear polymers show very good agreement with measured rheological data, indicating that the modeling validation is successful for the symmetric H-shaped polymers. We then test the hierarchical model further using literature data for symmetric H-PBds, for which the TGIC and experimental rheology data were published. We find that as long as the polymer composition is accurately determined, the hierarchical model can calculate the rheological behavior accurately. The theory can therefore be used to help to identify the composition or impurities, which are almost always present at low levels at least in such topologically complex samples.

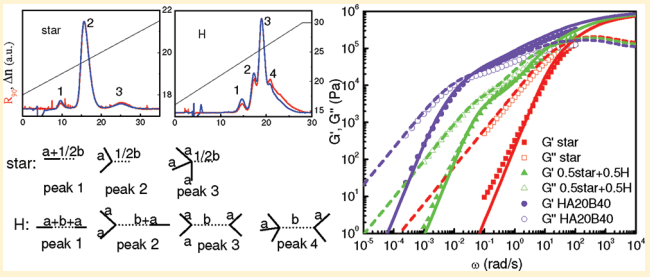

1. INTRODUCTION

Long chain branching is found in a large fraction of the polymers that are made and used commercially, particularly polyolefins, which is the highest-volume class of synthetic macromolecules manufactured worldwide. Previous studies indicate that it is often difficult or impossible to characterize low levels of long-chain branching from characterization methods other than rheology.[1] Although linear viscoelastic properties are sensitive to polydispersity and long-chain branching, rheological data alone do not directly reveal such information quantitatively. Such information could be obtained, in principle, however, by using molecular rheological theory to infer branching information from rheology. Fortunately, modern "tube theories" have greatly advanced our understanding of the relaxation dynamics and rheology of macromolecules with various branched architectures, such as star-shaped polymers with multiple arms of identical or different lengths.[2] However, understanding remains incomplete regarding the relaxation of complex branching structures in entangled polymer melts with multiple branch points, such as H- or comb-shaped polymers, especially for polymers with branches of differing lengths, such as asymmetric H polymers.

As the simplest species that contains two branching points, H-shaped polymers of polystyrene, polyisoprene, or polybutadiene have been previously studied rheologically by various research groups, and the data were used to test the accuracy of appropriate tube models for these structures.[3−8] However, the tube theory cannot be truly tested unless the polymer is completely pure or unless the topology, molar mass, weight fraction, and polydispersity of each component in the sample are well determined. It is thus significant that recent temperature gradient interaction chromatography (TGIC)[9] analysis of anionically synthesized H-shaped polybutadiene (PBd) polymers has shown that such samples can contain substantial amounts of branched byproducts of both low and high molar mass, whose presence is not always evident in more conventional size exclusion chromatography (SEC) traces.[8,10] Taking account of the real polymer structural distributions in such samples is obviously essential to assess the true accuracy of the model predictions. Chambon et al.[11] recently combined TGIC analysis with rheological measurements and rheological modeling to determine the distribution of numbers of branches in an anionically synthesized comb polymer, thus showing the potential power of combining TGIC with rheological analysis of branched polymers.

Received: May 18, 2011
Revised: July 21, 2011
Published: September 07, 2011

In this work, we describe the synthesis of a symmetric H polymer "HA20B40" and its characterization by TGIC. To be confident about the structure of each component in the final product, we also perform TGIC analysis of a precursor symmetric star polymer to help infer the possible structures in the final products. After validating our model on this cleanest sample, we analyze data on some previously studied symmetric H samples which were also well characterized by TGIC, but for which structures in the final products were inferred in part from assessment of the likely byproducts of the synthesis.[10] Here, we use a rheological model, the hierarchical model[12] to help infer the most likely structures in these literature H samples. We also test the robustness of our methods by also comparing another publically available model, the BOB (Branch-On-Branch) model,[13] with some of the rheological data. This paper is organized as follows: Section 2 describes the materials and experimental methods. In section 3, we describe the hierarchical model and modeling details. In section 4, we present and discuss our synthesis products, molecular characterization results, experimental rheological measurements, and the hierarchical model calculations. We also describe modeling of other H-shaped PBds from the literature to further test our theory. In particular, we show that the hierarchical model not only yields quantitative predictions for our symmetric H and its blends with star or linear polymers but also helps to identify the impurities in the sample. Conclusions and perspectives are drawn in section 5.

2. MATERIALS AND EXPERIMENTAL METHODS

2.1. Materials and Blends Preparation. Three 1,4-polybutadiene polymers, namely a linear, a star (1/2H), and a symmetric H polymer, as well as blends of these, were investigated. The chemical composition of cis-1,4, trans-1,4, and 1,2-vinyl was found to be 52%, 42%, and 6%, respectively. The linear PBd was purchased from Polysciences Inc. Its weight-average molecular weight and molecular weight distribution are 22.6 kg/mol and 1.05, respectively, provided by Polysciences Inc. As discussed below, this characterization was confirmed by comparison of its rheology with rheological predictions of the hierarchical model, which has been shown to be accurate for linear polymers. The three-armed symmetric star or 1/2H, which is an intermediate in the synthesis of the symmetric H-PBd, has three identical arms of targeted molar mass of 20 kg/mol. The targeted H-PBd sample is named according to the target molar masses of the arms and cross-bars; e.g., "HA20B40" denotes a sample with four arms of equal molar mass of 20 kg/mol and a backbone with a molar mass of 40 kg/mol.

Two kinds of blends, i.e., a blend of 50% weight fraction of HA20B40 with 50% weight fraction of the star (1/2H) and a blend of 50% weight fraction of HA20B40 with 50% weight fraction of the linear PBd, were designed. These two blends were prepared by dissolution of the polymers in toluene that was filtered with 0.2 μm pore-size sterile filters and then placed in a fume hood for about a week for initial evaporation of the solvent. The samples were then dried under vacuum at room temperature for another 2 weeks or more to ensure removal of the excess toluene. Two methods were used to determine the complete removal of the excess toluene: (1) no toluene smell after drying under vacuum; (2) the weight of the sample remains constant over a period of 3 days. The blends after drying were stored in a refrigerator ready for rheological measurements.

2.2. Synthesis and Purification. Synthesis of symmetric H-shaped PBd has been described in detail in previous publication.[14] Briefly, the synthetic steps shown in Figure 1 involve (a) growing a living PBd chain using *s*-BuLi as initiator in benzene at room temperature, (b) titration of 4-(dichloromethylsilyl)diphenylethylene with living PBdLi,

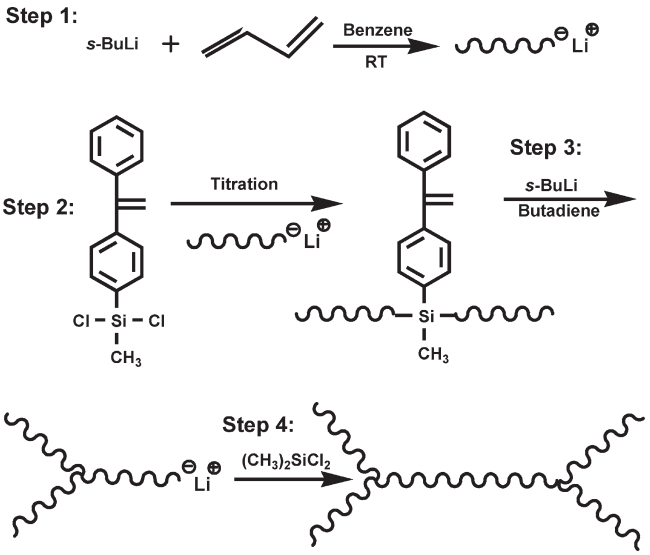

Figure 1. Synthetic steps of H-shaped polybutadienes.

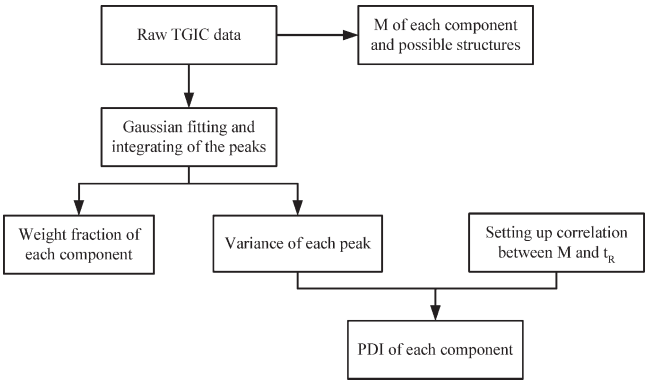

Figure 2. Method to characterize sample for model predictions.

(c) addition of *s*-BuLi to activate the double bond of diphenylethylene, (d) subsequent addition of butadiene to generate a living "1/2H", which has two arms and half of the final cross-bar, and (e) finally coupling the two "1/2H" molecules with dichlorodimethylsilane to produce an H-PBd, which has two arms attached to each end of the cross-bar. The raw final polymers were stabilized with butylated hydroxytoluene and precipitated into a large excess of methanol. Fractionation was performed using toluene/methanol as the solvent/nonsolvent pair. Fractionation was repeated to obtain optimal results. The fractionated polymer was precipitated in an excess of methanol and vacuum-dried prior to characterization.

2.3. SEC and TGIC Characterizations. A SEC apparatus equipped with a Wyatt miniDAWN LS detector with 60 mW power at a wavelength of 658 nm and a Shodex RI-101 RI detector with two PLgel mixed-C columns (300 × 7.5 mm, 5 μm) were used to characterize precursors and final H polymers. This characterization was performed at 40 °C with THF as the mobile phase at a flow rate of 0.8 mL/min; dn/dc was 0.128 mL/g.

The TGIC separations were carried out using a standard high-performance liquid chromatography (HPLC) system equipped with a C18 bonded silica column (AkzoNobel, Kromasil, 300 Å pore, 150 mm × 4.6 mm, 5 μm particle size); the mobile phase was 1,4-dioxane at a flow rate of 0.5 mL/min, and dn/dc was 0.095 mL/g. The system was

equipped online with a Wyatt miniDAWN LS detector and a Shodex RI-101 RI detector. The column temperature was programmed from 18−30 °C to cover the range of molar mass of each sample.

2.4. Further TGIC Analysis. The raw TGIC data provide us with the molar mass of each component in the sample, and on the basis of the synthesis mechanism, we can infer the possible structures of each peak as shown in Figure 7 (details discussed in section 4). However, in addition to information on molar mass of each peak, the weight fractions and polydispersity indexes (PDI's) are needed as inputs for theoretical predictions of rheology. The TGIC data shown in Figure 5 allow us to estimate the concentration and PDI of the main products as well as byproducts in the 1/2H (star) and HA20B40 PBd. The method for obtaining this information is summarized in Figure 2. Refractive index signals, Δn, were first deconvoluted using peak integration and Gaussian fitting to calculate the weight fraction of each component and the variance of each peak, σ^2_{peak}. Since TGIC retention time, t_R, and molar mass, M, can be approximated to be linearly correlated over a narrow molar mass range,[15] a correlation between M and t_R in the form of $M = a \times t_R + b$ can be set up, where a and b are constants, respectively. From eqs 1 and 2, the PDI of each component, assuming a normal distribution, can be calculated:

$$\sigma_M{}^2 = \sigma_{peak}{}^2 a^2 \quad (1)$$

$$\mathrm{PDI} = 1 + \frac{\sigma_M{}^2}{M^2} \quad (2)$$

where $\sigma_M{}^2$ is the variance of the molar mass, $\sigma_{peak}{}^2$ is the variance of each refractive index peak in TGIC figures, and M is the molar mass.

2.5. Rheological Experiments. The very viscous, "solidlike" samples, i.e. HA20B40 and the blend of HA20B40 with the 1/2H, were compression-molded into circular disks of 25 mm diameter and around 1.2 mm in height on a hot press. The less viscous "liquidlike" samples, i.e. 1/2H (star), linear, and the blend of HA20B40 with linear, were loaded onto the bottom plate of the 25 mm parallel plate geometry directly. Then the bottom plate with the sample was placed into a vacuum oven at room temperature under vacuum to get rid of the air bubbles trapped in the "liquidlike" samples.

For each sample, linear viscoelastic measurements were performed on an ARES strain-controlled rheometer with a 25 mm parallel plate geometry and around 1 mm gap. Dynamic strain sweep measurements were first conducted to select the strains in the range of linear response. Dynamic frequency sweep tests with the selected strains were conducted at a constant temperature of 25 °C with frequency sweeps from 0.0001 to 100 rad/s. In order to ensure sample stability, a nitrogen measurement atmosphere and added antioxidant were applied. In all cases, the terminal region was reached.

3. THEORY AND MODELING

The model we wish to validate and use for inferring most likely component structures in the sample is the hierarchical model (v3).[12] This hierarchical model has been previously successfully validated on linear, symmetric star, "T", and "Y" shaped asymmetric star, linear−linear blends, linear−star blends, and commercial metallocene polyethylene copolymers which are characterized by SEC.[2,12,16−19] Here we will validate this hierarchical model (v3) on a relatively "clean" H-shaped PBd (HA20B40), characterized by a more sensitive and accurate characterization tool (TGIC), and on its blends with linear and star polymers.

According to the concept of polymer hierarchical relaxation,[20−22] for a symmetric H-shaped polymer, as shown in Figure 3, immediately after a small step strain, only the arms can relax inward from their tips. Later, after the four identical arms are fully relaxed, these

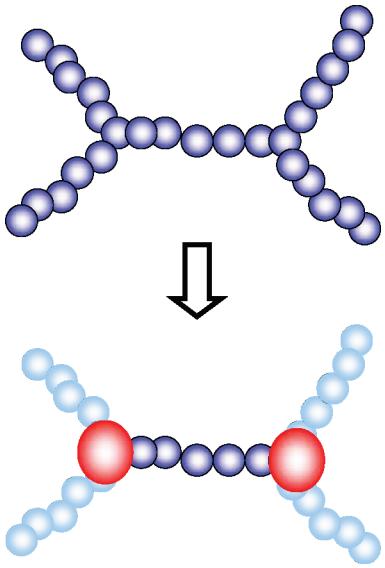

Figure 3. Conceptualization of algorithm for computing hierarchical relaxation of a symmetric H-shaped polymer.

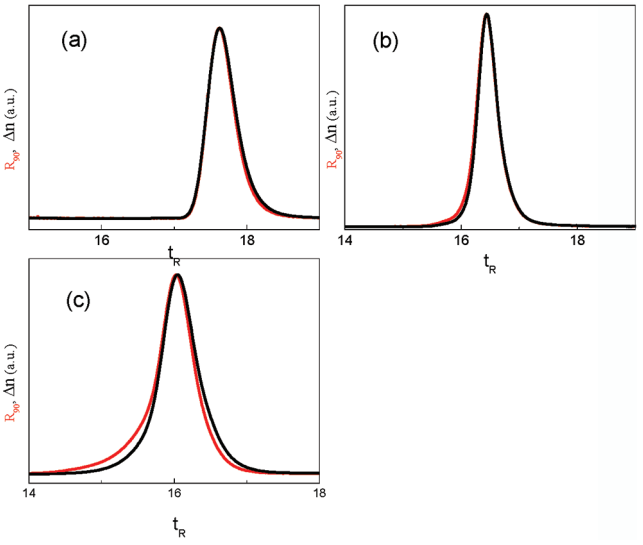

Figure 4. SEC (RI−Δn and LS at 90°−R_{90}) elution profiles of precursors and H-shaped PBd: (a) linear PBd arm, (b) star PBd (1/2 H), and (c) fractionated H-PBd (HA20B40).

arms are conceptually replaced by a frictional bead at the branch point at each end of the backbone. The unrelaxed molecule finally thus becomes conceptually a linear chain with a branch point at each end, illustrated in Figure 3b. The final relaxation then occurs by arm retractions and reptation of an effectively "linear" chain. The beads incorporate the friction added to the chain backbone by the side branches. A detailed description of this model is given elsewhere.[12]

To predict the rheological behaviors of our samples, we use the default parameters of the hierarchical model, that is, α = 4/3 and p^2 = 1/12, where α is dilution exponent and p^2 is coefficient of branch-point drag. Two of the material-dependent tube model parameters used here, namely the plateau modulus G^0_N and the entanglement molecular weight M_e, were taken from previous reported values for 1,4-PBd;[12] that is, G^0_N = 1.095 MPa

dx.doi.org/10.1021/ma2011377 |Macromolecules 2011, 44, 7799–7809

Table 1. SEC and TGIC Characterization of Final HA20B40 and Its Precursors, i.e. the Linear (the Arm of H) and the Star (1/2H)

	M_{w_arm}[a] (kg/mol)	M_{w_total}[a] (kg/mol)	PDI[a]	M_{peaks}[b] (kg/mol) peak 1	peak 2	peak 3	peak 4
linear (arm of H)	19		1.01	19			
star (1/2H)	19	58	1.03	38.5	54.8	73.6	
HA20B40	19	111	1.07	71	95	114	129

[a] Characterized by SEC. [b] Characterized by TGIC.

and M_e = 1620 g/mol. The definition of the entanglement molecular weight M_e used here is $M_e = 4/5 \times \rho RT/G_N^0$. Another tube model parameter, the frictional equilibration time τ_e, is obtained by fitting the value to the experimental rheology data for star (1/2H) and linear PBds studied in this work, which gives a value of $\tau_e = 5 \times 10^{-7}$ s. We then use these values of the three tube model parameters for modeling predictions on all the materials studied here, including HA20B40, literature H-PBds synthesized in the Mays' lab, and the star and linear PBds, without any adjustment. We note here that values of τ_e seem to be sensitive to synthesis details, and the best-fit value varies from lab to lab, as we will discuss in a future publication. Our preliminary simulation results indicate that the so-called "thin-tube" option and "arm-frozen" option[12] of the hierarchical model (v3) yield very similar results for the same tube model parameters because each component of the sample is nearly monodisperse after fractionation and purification. Therefore, we use "arm-frozen" option for all our predictions.

4. RESULTS AND DISCUSSION

4.1. SEC and TGIC Characterization Results. Figure 4 shows the SEC chromatogram for the symmetric HA20B40 and its precursors. SEC chromatograms recorded by a RI and LS detector shows one dominant peak for the linear PBd arm, the star (1/2H), and the fractionated HA20B40. The absolute molar masses determined from SEC-LS and summarized in Table 1 are in good agreement with the target molar masses of HA20B40 and its precursors. The narrow PDI values ranging from 1.01 to 1.07 also suggest that these samples are quite uniform albeit some polydispersity in H-PBd is noticeable from the mismatch of RI and LS signals. However, this does not necessarily mean that these samples are free from any side product. Specially, a small amount of byproduct with different branching degree cannot be detected by conventional SEC-LS. This is an expected behavior of SEC, which only separates the polymer chains based on their hydrodynamic volume.[23,24] Thus, more precise characterization using an advanced technique such as TGIC is required to identify these materials and their architecture.

TGIC is an interaction chromatography technique that has much superior resolution to SEC.[25] Additionally, TGIC separation of polymer molecules is driven by an enthalpic interaction of the solute molecules with the stationary phase, and this interaction is varied by changing the column temperature during the elution.[15] Thus, TGIC retention is sensitive to the molecular weight while being less sensitive to the chain architecture. TGIC can resolve byproduct species of the linking reaction, such as coupled arms, stars, and H-molecules, if they have different molecular weight.[8] SEC cannot do the same since hydrodynamic volume of branched polymers does not change with molar mass

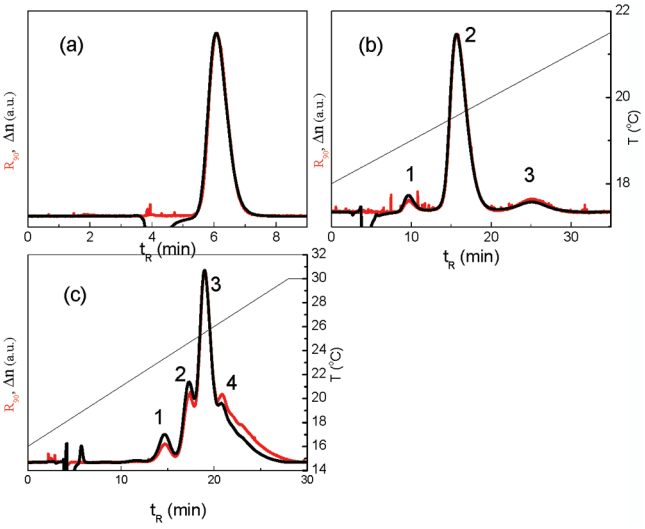

Figure 5. TGIC of (a) linear PBd arm (18 °C isothermal), (b) star PBd (1/2H), and (c) fractionated H-PBd (HA20B40).

as sensitively as linear polymers. Thus, we used TGIC for a detailed characterization of our H-molecules and its precursors. In Figure 5a, a TGIC chromatogram of a linear PBd arm is displayed. The separation was carried out under isothermal conditions at 18 °C and the TGIC chromatogram shows one dominant peak, just as does SEC (Figure 4a). Precise match of RI and LS signals indicates that the linear PBd arm has a very narrow molar mass distribution.[25] Such an isothermal elution is possible for polymers with a very narrow molar mass distribution. For polymers with broad molar mass distribution, a temperature program is necessary since the IC retention increases with molar mass exponentially.[15] With a temperature program ranging over 18−21.5 °C in 35 min, a star (1/2H) sample made by multiple synthetic steps shows three clearly resolved peaks labeled as 1, 2, and 3 in Figure 5b. The molecular characteristics of the three different peaks summarized in Table 1 are in good agreement with our expected values. The side products are responsible for the slight mismatch of RI and LS signal in the SEC analysis (Figure 4b), but it is often neglected in SEC analyses.

Similarly, TGIC of HA20B40 shows four distinct peaks in Figure 5c. The molar masses of the peaks 1−4, summarized in Table 1, are in good agreement with the total molar masses of HA20B40 and its precursors. The possible structures corresponding to the TGIC peaks are discussed in the next section.

4.2. Inference of Possible Byproduct Structures Based on TGIC and Synthesis Mechanism. Based on the reaction mechanism of Figure 1, the possible products that can form during the synthesis of star (1/2H) and HA20B40 are shown in Figure 6. The step-by-step analysis with SEC-LS and TGIC also confirmed that these are the possible structure in our samples. For example, the TGIC chromatogram in Figure 5 shows three peaks for star (1/2H) (Figure 5b) and four peaks for purified HA20B40 (Figure 5c). The molar mass of peak 2 in Figure 5b is 54.8 kg/mol, which is 3 times higher than the molar mass of a linear arm (Table 1). This means peak 2 is our desired 3-arm star (1/2H). Similarly, the peak 1 molar mass of 38.5 kg/mol and peak 3 molar mass of 73.6 kg/mol correspond to two- and four-arms star, respectively. The likely structures corresponding to the three TGIC peaks of Figure 5b are shown in Figure 7a.

HA20B40 shows four TGIC peaks in Figure 5c. The molar masses of peaks 1−4 are summarized in Table 1. On the basis of

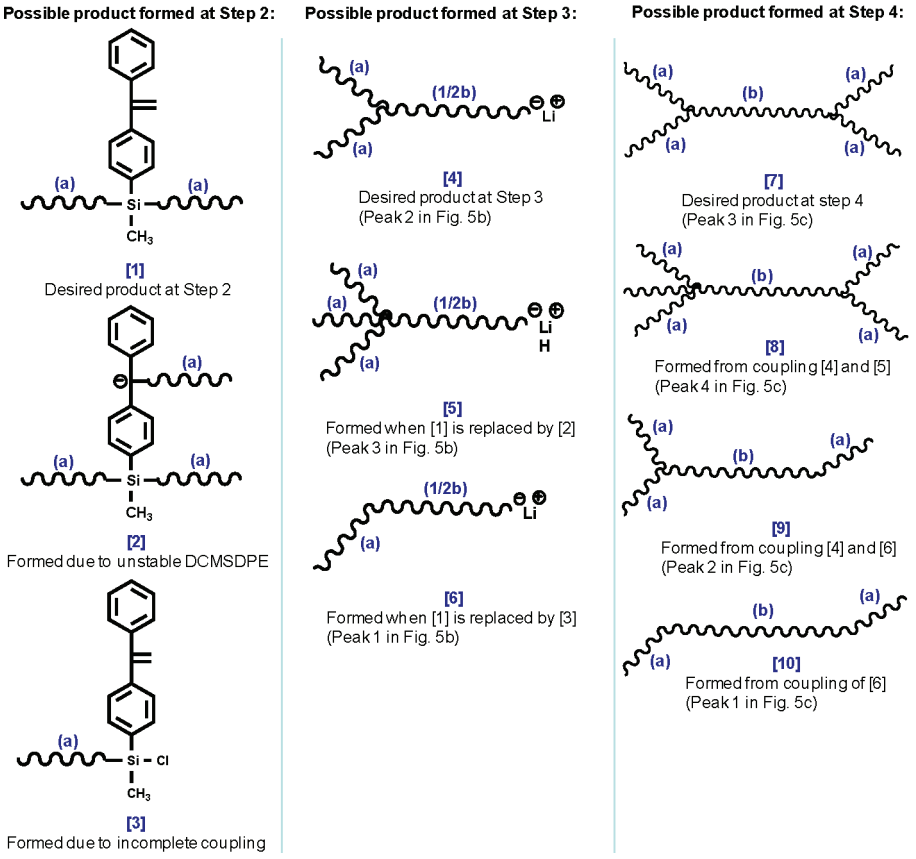

Figure 6. The most possible product and byproducts formed in the star (1/2H) and HA20B40 synthesis. The length of each segment is shown in parentheses with *a* equal to the arm length and *b* equal to the length of a cross-bar.

the reaction mechanism[10,14] and the known molar mass of HA20B40s precursor, we can confidently identify all these four peaks and their structures, which are given in Figure 7b.

4.3. Further Analysis of TGIC Data. Based on the method described in section 2.4, the molecular characteristics of each component in the star (1/2H) and HA20B40 samples are summarized in Tables 2 and 3, and the possible structures corresponding to each peak are shown previously in Figure 7. The PDI of each component (or peak) for the star (1/2H) and HA20B40 are calculated to be ranging from 1.00 to 1.02; i.e., each component is a single species composed of anionic-polymerized polymer chains.[26] For the star PBd, the main product takes up about 84% of the total weight, and is nearly symmetric, with two arms having molar masses of 19 kg/mol, and the third arm, which is a half of the backbone in the H polymer, has nearly the same molar mass. As described in section 2.2, we use this unfractionated star to make the H, and we also reserved some of the unfractionated star for rheological studies. For the HA20B40, we purified the sample by conventional fractionation using toluene/methanol as the solvent/nonsolvent pair and used the purified sample for our rheology study. However, even after purification, the target product of HA20B40 has a weight fraction of only about 50%, which is, however, higher than the content (36.4%) of targeted H polymer in the sample synthesized by Perny et al.[8]

4.4. Experimental and Theoretical Linear Viscoelastic Properties of HA20B40 and Its Blends with Linear or Star PBds. By applying the rheological measurement method described in section 2.5, the experimental linear viscoelastic properties of the purified HA20B40, unfractionated star (1/2H), and linear polymers and their blends at 25 °C are shown in Figure 8 (H, star, and a 50/50 blend of the two) and Figure 9 (H, linear, and a 50/50 blend

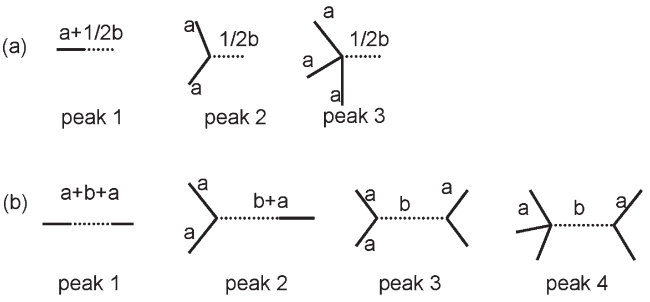

Figure 7. Possible structures of (a) star (1/2H) and (b) HA20B40 based on the TGIC.

Table 2. Further TGIC Data Analysis of the Star (1/2H) PBd

peak	peak type	weight fraction%	σ^2_{peak}	M (kg/mol)	a^a	$\sigma^2_M \times 10^{-7}$	PDI
1	Gaussian	5.3	0.39	38.5	2262.4	0.20	1.00
2	Gaussian	83.6	0.98	54.8	2262.4	0.50	1.00
3	Gaussian	11.1	3.88	73.6	2262.4	1.98	1.00

[a] *a* is the prefactor in the correlation $M = 2262.4 \times t_R + 17664$ with $R^2 = 0.9924$.

dx.doi.org/10.1021/ma2011377 |*Macromolecules* 2011, 44, 7799–7809

Table 3. Further TGIC Data Analysis of HA20B40 PBd

peak	peak type	weight fraction (%)	σ^2_{peak}	M (kg/mol)	a^a	$\sigma^2_M \times 10^{-7}$	PDI
1	Gaussian	7.8	0.38	71	9653.5	3.53	1.01
2	Gaussian	16.8	0.28	95	9653.5	2.63	1.00
3	Gaussian	50.2	0.41	114	9653.5	3.79	1.00
4	Gaussian	25.1	0.73	129	9653.5	6.84	1.00

[a] a is the prefactor in the correlation $M = 9653.5 \times t_R - 70900$ with $R^2 = 0.9973$.

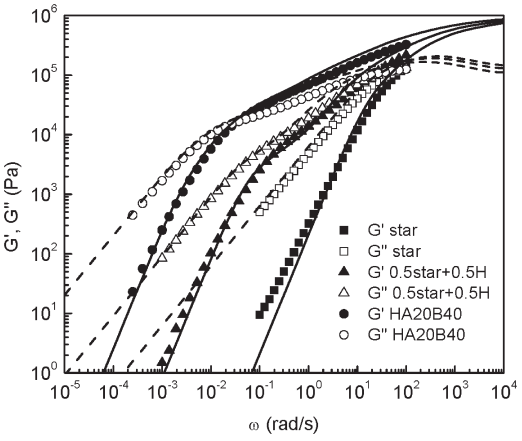

Figure 8. Experimental storage modulus G' and loss modulus G'' data, and hierarchical model calculations for purified HA20B40, unpurified star (1/2H), and a 50/50 (by weight) blend of the two. Solid symbols (solid lines) and open symbols (dashed lines) are experimental data (theoretical predictions) for G' and G'', respectively.

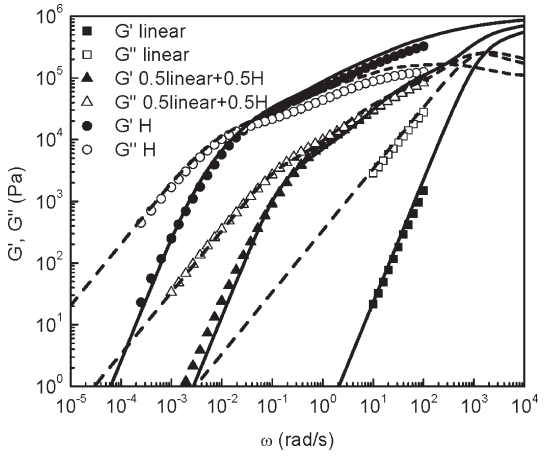

Figure 9. Experimental storage modulus G' and loss modulus G'' data and hierarchical model calculations for purified HA20B40, linear PBds, and their 50/50 blend. Solid symbols (solid lines) and open symbols (dashed lines) are experimental data (theoretical predictions) for G' and G''.

of the two) (the symbols are the experimental data). Here, "H" actually refers to the mixture of architectures described in Table 3, and "star" means the mixture described in Table 2. As expected, in Figure 8, the blend of star and H relaxes faster than the unblended HA20B40 and slower than the unblended star (1/2H) PBd. Similar behaviors are shown in Figure 9. In all the cases

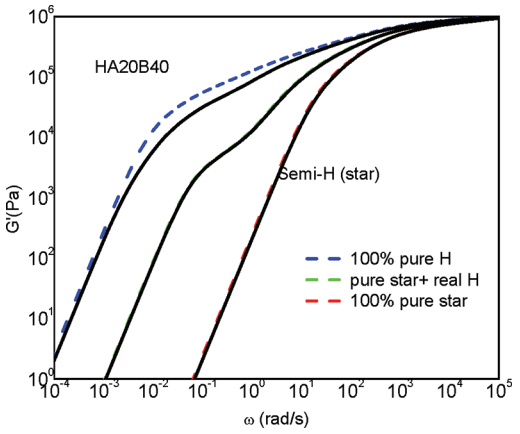

Figure 10. Determination of the effect of impurities on the rheology of the synthesized semi-H and HA20B40 materials by comparing the predictions of 100% pure materials with the predictions for the actual materials containing the measured concentrations of impurities. The blue dashed line is the prediction of G' for 100% pure HA20B40; the red dashed line is the prediction of G' for 100% pure star; and the green dashed line is the prediction of G' for the 50/50 blend of 100% pure star and real HA20B40. The black solid lines are the predictions of G' for the real materials.

here, the terminal region has been reached during the rheological testing.

The molar mass, weight fraction, polydispersity, and possible structure of each component in the synthesized materials have been determined as described and tabulated above. Because the star (1/2H) precursor and the final H polymer were characterized by TGIC, we can be confident of the assigned structures of each component in HA20B40. We believe that this is the first time that both the precursor and the final product were characterized by both TGIC and rheological studies. This increases our confidence in the characterization of product and the rheological modeling, the latter of which must match rheological data for both the precursor 1/2H (star) polymer and the final product, HA20B40.

Our accurate determination of the molecular characteristics of each component, i.e. molar mass, weight fraction, polydispersity, and likely structure, make it possible for us to do the modeling work accurately. We use the hierarchical model to calculate the rheological behaviors of unblended and blended melts. As shown in Figure 8 (H, star, and their 50/50 blends) and Figure 9 (H, linear, and their 50/50 blend), the rheology of these very well-characterized samples (HA20B40, 1/2H, and the linear PBds) are quite well predicted by the theory. Furthermore, when we deliberately add additional well-characterized star or linear polymers into HA20B40 to mimic the effect of impurities, we can predict the effect of this on the rheology of the 50/50 star-H blend as shown in Figure 8 and the 50/50 linear-H blend as shown in Figure 9.

To determine the effects of impurities on the rheology of the star (1/2H) and HA20B40, we predicted their rheological behaviors theoretically with and without the impurities. As shown in Figure 10, for the star (1/2H), which contains about 84 wt % targeted star molecule, the rheology is predicted to be almost identical to that of a 100% pure sample (the red dashed line). However, we cannot easily say that the star sample is pure enough only based on this observation, since the rheology of pure stars might not be very sensitive to polydispersity from the natural narrowing of constraint release in these systems. Therefore, we also predicted the rheological behavior of a 50/50 blend

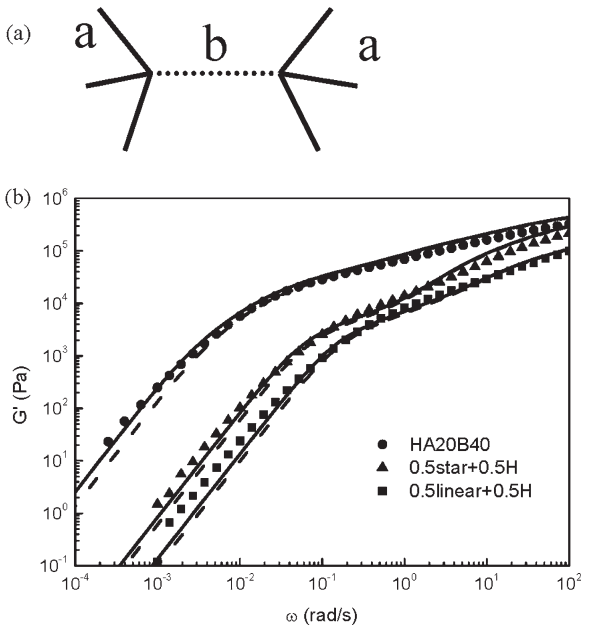

Figure 11. (a) A possible pom-pom-shaped molecule present in the tail of peak 4 of Figure 5c. (b) The rheological predictions obtained by assuming that peak 4 is entirely this pom-pom-shaped molecule (dashed lines) compared to the predictions obtained when it is assumed that it is entirely the 5-armed structure (solid lines) in Figure 5b, peak 4.

of pure star and real HA20B40 (green dashed line). As shown in Figure 10, the theoretical prediction is also almost identical to that of the real 50/50 star-H blend, indicating that the impurities in the star are small enough not only to have little effect on the rheology of the 100% star but also to have little effect when this star is blended with an H polymer. For the HA20B40, however, the impurities accelerate the terminal relaxation by about a factor of 2, which affects the rheology in the low-frequency region below 1 rad/s.

Furthermore, the long tail of peak 4 in Figure 5c indicates that additional higher-molecular-weight components might be present in the material. Based on the synthesis mechanism, the most likely larger component is the pom-pom-shaped molecule, shown in Figure 11a, which is formed by coupling of two 4-armed stars of peak 3 in Figure 7a. Since the weight fraction of this possible pom-pom molecule cannot be determined from the TGIC characterization described here, it is not possible to determine accurately effects of this pom-pom molecule on the rheology. However, to estimate the maximum effect that this component might have on the rheology, we can assume that peak 4 in Figure 5c consists entirely of this pom-pom polymer, although this is an exaggeration because the average molar mass of peak 4 is too low to be consistent with this peak being entirely a pom-pom polymer. Nevertheless, Figure 11b shows that the theoretical prediction obtained by assuming that peak 4 is composed entirely of this pom-pom-shaped molecule is not significantly different from the prediction obtained by assuming that peak 4 is entirely the 5-armed structure shown in Figure 7b. Therefore, the long tail of peak 4 does not have significant effects on the rheological behavior of this melt or of its blends with star polymer.

4.5. Identification of Possible Structures in Other H-Shaped Polymers Using the Hierarchical Model. Recently, SEC data, TGIC data,[10] and experimental linear viscoelastic data[27] were published for four symmetric H-shaped PBds, namely

Table 4. Estimated Structures and Compositions of HA12B40, HA12B100, HA30B40, and HA40B40 (Table 4 in Ref 10)

sample	peak	M (kg/mol)	PDI	wt %	inferred structure
HA12B40	1	22	1.01	3	linear
	2	29	1	6	linear
	3	43	1.01	15	linear or 3-arm star
	4	55	1	21	4-arm star
	5	69	1.01	25	3-arm star
	6	79	1.01	30	H
HA12B100	1	103	1.02	33	linear or 3-arm star
	2	168	1.01	15	3-arm star
	3	187	1.02	52	H
HA30B40	1	83	1.01	18	linear or 3-arm star
	2	108	1.01	21	4-arm star
	3	138	1	27	3-arm star
	4	167	1	34	H
HA40B40	1	113	1.01	6	linear or 3-arm star
	2	129	1.01	17	3-arm star
	3	205	1	77	H

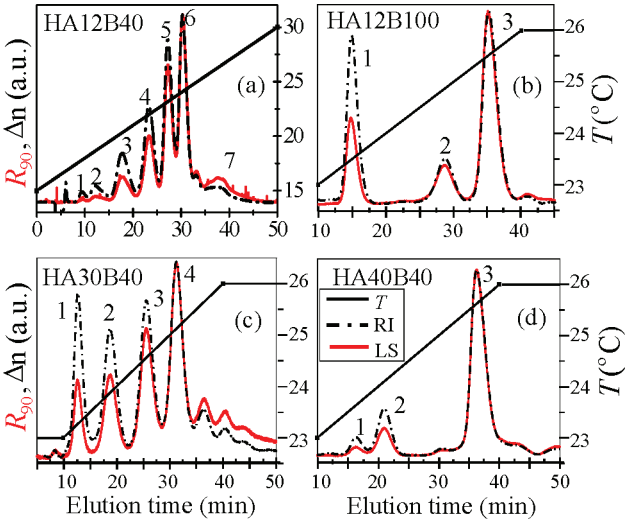

Figure 12. TGIC chromatograms of HA12B40, HA12B100, HA30B40, and HA40B40 (from Figure 5 in ref 10). In this figure, "RI" means "refractive index", corresponding to the refractive index signal, Δn, detected by a Shodex RI-101 RI detector. "LS" means "light scattering", corresponding to the light scattering signal, R_{90}, detected by the Wyatt miniDAWN LS detector. The refractive index signal, Δn, is used here in our study to estimate the mass fraction corresponding to each peak.

HA12B40, HA12B100, HA30B40, and HA40B40, synthesized by Mays' group,[14] using a method similar to that used to synthesize HA20B40, the H polymer described in this paper. As mentioned in previous publication,[10] SEC techniques were unable to resolve the structural compositions of the long chain branched polymers containing various byproducts due to its inherent low resolution. We will therefore use the TGIC results for these samples to further test our rheological theory, using the same tube model parameters as used for HA20B40.

Table 4 (Table 4 in the previous publication[10]) summarizes the molecular characteristics of these four symmetric H-shaped

dx.doi.org/10.1021/ma2011377 |Macromolecules 2011, 44, 7799–7809

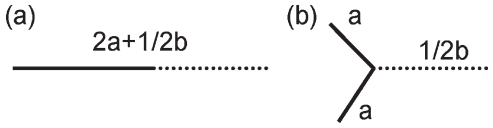

Figure 13. Inferred possible structures corresponding to peak 1 in Figure 12 for HA12B100 and HA40B40. (a) The inferred linear-shaped PBd with molar mass equal to the sum of that of the two arms and the half backbone of the H. (b) The inferred star-shaped PBd which has two identical arms each with molar mass equal to that of the arm of the H and one arm with molar mass equal to that of the half backbone of the H.

Table 5. Comparisons of the Molar Mass of Two Possible Structures with the Actual Molar Mass of Peak 1 for HA12B100 and HA40B40

	M_{arm} (kg/mol)	$M_{backbone}$ (kg/mol)	M_{linear} [a] (kg/mol)	M_{star} [b] (kg/mol)	M_{peak1} [c]
HA12B100	15.3	125.8	93.5	93.5	103
HA40B40	41.6	38.6	102.5	102.5	113

[a] Calculated using $M_{linear} = 2M_{arm} + {}^1/_2M_{backbone}$ [b] Calculated using $M_{star} = 2M_{arm} + {}^1/_2M_{backbone}$ [c] The molar mass of peak 1 from TGIC trace.

PBds. Figure 12 shows the TGIC data for these four H-shaped PBds, which corresponds to Figure 5 in the previous publication.[10] The peaks labeled in Figure 12, and the structures inferred for each peak, based on knowledge of the reaction chemistry, are listed in Table 4. As seen in Figure 12, HA12B100 and HA40B40 are the cleanest samples with the fewest byproducts. We therefore start with these two symmetric H PBds for our further model validation and possible byproduct structure determination.

The possible structures corresponding to "peak 1" in HA12B100 and in HA40B40 were each previously identified as either a linear or a three-armed star molecule[10] (see Table 4 and Figure 12). As shown in Figure 13, the possible linear-shaped PBd was inferred to be a combination of two arms and one-half backbone based on the synthesis mechanism and molar mass information characterized from TGIC, while the possible star-shaped PBd was inferred to have two identical arms with the molar mass of the arm of the H PBd and one arm with of molar mass of the half backbone.[10] We do not believe that the linear molecule is a reasonable reaction byproduct, but consider it here, because it was listed as a possible byproduct in the earlier publication.[10] The molar masses of these linear-shaped PBd and star-shaped PBd for HA12B100 and HA40B40 are listed in Table 5. These two structures have identical molar masses, both of which are close to that of peak 1.

Here, we use our hierarchical model with the model parameters described in section 3 to test these two possibilities. In each case, we retain the weight fractions, polydispersities, and identities of all other components of HA12B100 and HA40B40 the same (as given in Table 4). We take the molar mass corresponding to either the linear or star molecule from the molar mass assigned from the TGIC analysis, that is, M = 103 kg/mol for HA12B100 and M = 113 kg/mol for HA40B40. As shown in Figure 14, the modeling prediction for HA12B100 with peak 1 corresponding to a star-shaped molecule matches the experimental rheology data well, while the choice of a linear chain for peak 1 leads to prediction of a peak in G'' at a frequency corresponding to the inverse relaxation time of the linear chain.

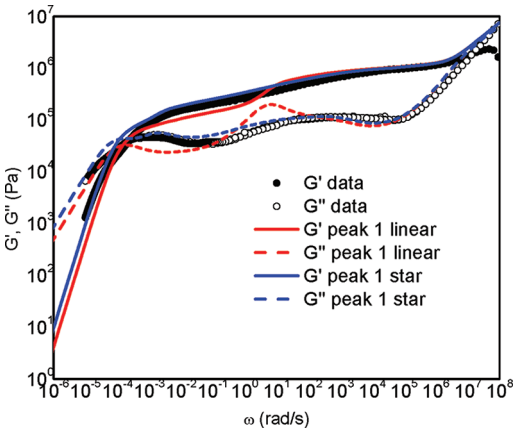

Figure 14. Effect of identity of peak 1 in HA12B100 on rheological predictions from the hierarchical model compared with experimental rheology data. Solid symbols (open symbols) are experimental G' (G'') data. The red solid line (dashed line) is the theoretical calculation of G' (G'') assuming peak 1 is a linear-shaped PBd, while the blue solid line (dashed line) assumes that peak 1 is star-shaped PBd for G' (G'').

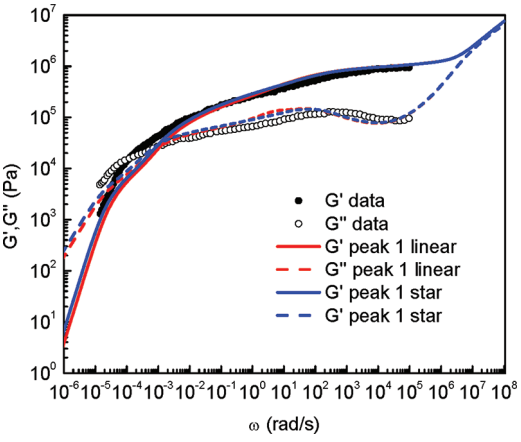

Figure 15. The same as Figure 14, except for HA40B40. As in Figure 14, the red solid line (dashed line) is the theoretical calculation of G' (G'') assuming peak 1 corresponds to a linear molecule, while the blue solid line (dashed line) assumes it is a star.

Since this peak is not observed experimentally, the choice of a star structure for peak 1 is more likely to be the correct assignment. (As noted above, this choice is also the more likely one based on the chemical synthesis.) Thus, the prediction of the rheological theory is sensitive to the component structure, *even when the possible structures have the same molar mass.* Therefore, in addition to TGIC characterization, theoretical modeling may be useful to determine or confirm the correct identification of impurities in the melt.

Similarly, by using the hierarchical model with the same model parameters, we test the two suggested possibilities for the components of HA40B40 as shown in Figure 15. Because of the small weight fraction for peak 1 in HA40B40, these two structure possibilities do not generate a significant difference in the predicted linear viscoelasticity. (However, the synthesis makes the star the more likely correct choice for this peak.)

So far, we have validated the hierarchical model using the well-characterized H sample HA20B40, for which we obtained TGIC data not only on the final product but also on the intermediate to

dx.doi.org/10.1021/ma2011377 |*Macromolecules* 2011, 44, 7799–7809

Table 6. Characterization of HA12B40 PBd

peak	peak type	weight fraction (%)	σ^2_{peak}	M (kg/mol)	a^a	$\sigma^2_M \times 10^{-7}$	PDI
1	Gaussian	1.5	0.22	22	5147	0.59	1.01
2	Gaussian	3.4	0.54	29	5147	1.44	1.02
3	Gaussian	10.8	0.51	43	5147	1.36	1.01
4	Gaussian	18.4	0.32	55	5147	0.84	1.00
5	Gaussian	24.9	0.27	69	5147	0.71	1.00
6	Gaussian	34.2	0.26	79	5147	0.69	1.00
7	Gaussian	6.8	1.39	96.2[b]	5147	3.69	1.00

[a] a is the prefactor in the correlation $M = 5147 \times t_R - 12569$ with $R^2 = 0.9897$. [b] M of peak 7 was calculated based on the correlation between M and t_R

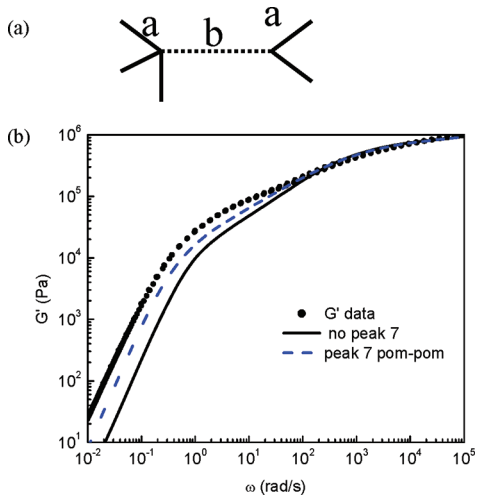

Figure 16. (a) Estimated possible structure of peak 7 in HA12B40. (b) Comparisons of hierarchical model predictions of G' assuming different possible structures of peak 7 in HA12B40. The solid line is the prediction without peak 7, the red dashed line is the prediction assuming peak 7 is star-shaped; the blue line assumes it is comb-shaped; and the green line assumes it is H-shaped.

increase our confidence about the identity of each component in the final product. We has also used this model to predict the rheological behaviors of previous published relatively "clean" H-shaped PBds, namely HA12B100 and HA40B40, and to help identify the most likely structure corresponding to one of the peaks in each of these materials. These successes in modeling symmetric H polymers give us confidence to proceed to analyze the more complex melts HA12B40 and HA30B40, which have more components (peaks) in their TGIC chromatograms.

As summarized in Table 4, HA12B40 was reported to have six components in a previous publication.[10] However, as can be seen in Figure 12, there is another (seventh) broad peak corresponding to elution times ranging from 35 to 40 min, labeled as peak 7 in the figure. By using the further analysis method on TGIC results described in section 2.4, a correlation between M and t_R of HA12B40 can be established as shown in Table 6, and the molar mass of peak 7 can be estimated by using this correlation to be 96 kg/mol. Once we add this seventh component, the weight fraction of the other components must be adjusted so that the total equals 100%. Based on the synthesis mechanism,[10,14] the suggested structure of peak 7 is shown in Figure 16a. The rheological predictions corresponding to these are shown in Figure 16b. Please note here, as previously inferred,[10] that peak 3 of HA12B40 might be either a linear or a star-shaped PBd. Our preliminary results indicate that either a linear or star for peak 3 generates similar predicted rheology, but the synthesis makes the star the more likely correct choice for peak 3. Therefore, we assume peak 3 is a star-shaped PBd in the following work for our identification of peak 7. As we can see in Figure 16b, the choice for the high-molecular-weight component greatly improves the prediction over that obtained when this component is neglected. The tail after elution times of 40 min in Figure 12a might contain even higher MW side products, the inclusion of which make the fitting of the model to the rheological data even better.

The polymer in Figure 12c, HA30B40, contains large quantities of impurities as well as multiple unidentified high molar mass peaks. The predictions of the hierarchical model, using only the identified peaks, shows terminal relaxation at a frequency more than a decade larger than predicted (data not shown). Since identification of the multiple high molar mass peaks would rely largely on guesswork, we did not attempt to find a set of possible structures that might bring the predicted rheological response closer to what was observed.

Finally, we carried out similar predictions for both HA20B40 and for HA12B100 polymer using the BOB model with parameters used previously for 1,4-polybutadiene,[13] i.e., $\alpha = 1$, $p^2 = 1/40$, $G^0_N = 0.97$ MPa, $M_e = 1836$ g/mol, and $\tau_e = 2.75 \times 10^{-7}$ s, and found roughly similar, although not quite as good, agreement to that obtained by the hierarchical model.

5. CONCLUSIONS AND PERSPECTIVE

The advent of temperature gradient interaction chromatography (TGIC) as a refined characterization method has revealed that multistep synthesis of architecturally complex polymers, such as "H" polymers, typically leads to multiple side products that often go undetected or disregarded by conventional SEC analysis as mentioned in previous publications[8,10] and reported here. Thus, it is prudent to assume that such materials (H and comb polymers) reported on in the past, prior to the application of TGIC characterization, may also have contained such impurities, which went undetected. This might cast some doubt on previous studies, which used rheological data for such polymers to test rheological theories for long-chain-branched polymers. Indeed, the agreement of rheological predictions with experimental data for such materials has been "hit or miss", with good agreement being obtained in some cases, but with agreement being poor in other seemingly similar cases, unless parameters were arbitrarily adjusted.[6,7,28,29] Obviously, the testing and improvement of tube models are hindered by the uncertainty in composition of such materials, since failure of the theory to predict correctly the rheology could be attributed either to failure of the rheological model or to some undetected impurity in the material.

To address this serious problem, we here have brought to bear a combination of methodologies. These include (1) TGIC analysis of both the product H material and its synthetic precursor star polymer, (2) rheological characterization and modeling of both the product material and its precursor, and (3) rheological characterization and modeling of blends of the H material with star and linear polymers to demonstrate the ability of the rheological model to account for the rheological effects of substantial quantities of impurities. In this way, we believe that

we are able to develop a convincing demonstration that we have not only identified the impurities, but also can account for their effect on rheological properties.

In essence, this approach presented here abandons the traditional approach[11] to polymer rheological modeling, in which pristine, "monostructural" materials are targeted for synthesis and rheological measurement, in order to test rheological models in the simplified limit of ideal specimens. It has already been recognized for some time now that polymers with long-chain branching are so sensitive to polydispersity that even when SEC traces show nominal M_w/M_n values less than 1.05, or even 1.01, the samples must be treated as "polydisperse" samples for purposes of rheological modeling.[6] Furthermore, the polydispersity index determined by SEC was reported to be inaccurate for linear polymers with narrow distribution due to the band broadening of SEC.[25] The situation for branched polymers is even worse. The PDI value of branched polymers determined by SEC is entirely unreliable since SEC cannot separate branched polymers according to molecular weights. Therefore, SEC-based characterization of branched polymers, particularly those prepared by anionic polymerization targeting certain complex structure, is not at all sufficient.

We are here taking the next logical step by assuming that these samples are not only polydisperse in molar mass but are also structurally polydisperse. Thus, we claim that it may not be realistic to hope to carry out clean enough chemistry, or thorough enough fractionation, to drive this structural heterogeneity down to levels low enough to make it negligible. It may therefore be better, instead, to seek to measure the compositional heterogeneity accurately and account for it in rheological models. This step, though drastic, can actually be viewed optimistically as simply propelling theoretical work toward the ultimate goal of accounting for the compositional heterogeneity of commercially synthesized polymers. We are simply recognizing that even anionically synthesized polymers of complex architecture are almost invariably mixtures of different molar masses and different structures and therefore seek to account for the effects of the heterogeneous components on the rheology.

Following this paradigm, here we have combined knowledge of the synthesis mechanism, TGIC characterization, experimental rheology measurements, and advanced tube model predictions to identify the composition of anionically synthesized symmetric H shaped PBds and to determine the effect of impurities on their rheology.

Specifically, we here described the synthesis, purification, TGIC, and rheological characterization of a new, relatively "clean" symmetric H material, HA20B40, containing four distinct TGIC peaks in its chromatogram and with 50% of the mass of the material belonging to the intended H polymer structure. We also used TGIC to analyze the composition of the synthetic precursor to this H polymer, which was composed predominantly (i.e., 84%) of the intended symmetric star, with only two side peaks, both of whose structure could be readily identified from knowledge of the reaction chemistry. From this information, and knowledge of the reaction pathways, the composition of the final H product could be determined with high confidence. Feeding this composition into a tube model, the hierarchical model that accounts for the effects of multiple components on rheological predictions, we successfully predicted the rheology of both the symmetric star precursor material and of the final melt, using preassigned values of the rheological parameters. We also successfully predicted the rheology of a 50/50 blend of the symmetric H melt and the precursor nearly symmetric star as well as of a 50/50 blend of the symmetric H with a well-characterized linear polymer. All predictions agreed well with the data, confirming that the model is able to predict the rheology not only of symmetric H polymers but also of blends of the symmetric H polymer with star and linear materials, including star and linear contaminants that appear as reaction byproducts. We also showed, using rheological modeling, that the small level (16%) impurity in the star did not significantly affect the rheology, so that this star was "pure enough" for rheological work. However, the larger impurity level (50%) in the H shifted the relaxation in the terminal region by a factor of 2, according to the rheological model.

As a second step in this new direction for branched polymer characterization and rheological modeling, we re-examined four symmetric H polymers synthesized in the same lab, but for which characterization of the intermediate had not been performed and some of which contained even more impurities, or higher concentrations of them. In two cases (HA12B100 and HA40B40), only one of the peaks was uncertain and could be identified as either a linear or a star molecule. By comparing rheological predictions assuming either a linear or a star molecule, we identified the star structure as the most likely impurity in HA12B100. For HA40B40, on the other hand, we found that rheological testing was not sensitive to the star or linear identity of the impurity. An additional sample, HA12B40, showed an unidentified high molar mass peak, the neglect of which led to modestly inaccurate rheological predictions. Including any of three reasonably likely structures for this peak resulted in predictions in good agreement with the experimental rheology. For the fourth sample, HA30B40, there were multiple unidentified high molar mass peaks, and neglecting them, we obtained wildly inaccurate rheological predictions. In the case of HA30B40, the uncertainties in identity of these additional peaks precluded successful rheological modeling.

The approach we have initiated here suggests that in the future complex branched polymer synthesis, molar mass and structural characterization, rheological measurement, and rheological modeling might no longer be carried out separately, but rather in concert. Thus, the "characterization" will no longer considered complete until the rheological data have been compared to predictions of a rheological model. This approach is risky, since flaws in the rheological model could be covered over by misidentifying one or two peaks in the TGIC spectrum. We recommend that this risk be minimized by taking two additional steps. The first is to characterize not only the final product but also one or more complex synthetic intermediates, by both TGIC and rheology, to help more reliably identify impurities that show up in the final product and to provide more thorough validation of the rheological model. The second is to blend the final product with well-characterized linear and star molecules that are similar in molar mass to those of likely impurities. Only if the rheological model can accurately predict the effect of these on the rheology of the melt can the model be considered reliable enough to identify impurities in the product and account accurately for their effect on rheology.

We note that even these steps are probably not sufficient to identify the peaks present in materials as complex as HA30B40 or to account for their influence on rheology. However, in the future, it may be possible to fractionate such complex mixtures by preparatory TGIC in quantities large enough to perform rheological characterization on fractions corresponding to each peak. This may allow the high molar mass peaks to be identified.

If they could be identified, then tube models such as the hierarchical model could be tested even for branched melts with complex side products, such as those likely present in HA30B40. This would further advance a new methodology in which combining rheological testing and modeling with TGIC and other methods becomes an important means of characterizing the branching structures present in polyolefins.

AUTHOR INFORMATION

Corresponding Author
*E-mail: rlarson@umich.edu.

ACKNOWLEDGMENT

We acknowledge support from NSF under grants DMR 0906587 and DMR 0906893. Any opinions, findings, and conclusions or recommendations expressed in this material are those of the authors and do not necessarily reflect the views of the National Science Foundation (NSF). T.C. acknowledges the support of NRF via NRL (R0A-2007-000-20125-0), SRC (R11-2008-052-03002), and WCU (R31-2008-000-10059-0) programs.

REFERENCES

(1) Janzen, J.; Colby, R. H. *J. Mol. Struct.* **1999**, *485*, 569.
(2) Chen, X.; Larson, R. G. *Macromolecules* **2008**, *41*, 6871.
(3) Roovers, J.; Toporowski, P. M. *Macromolecules* **1981**, *14*, 1174.
(4) McLeish, T. C. B. *Macromolecules* **1988**, *21*, 1062.
(5) Hakiki, A.; Young, R. N.; Mcleish, T. C. B. *Macromolecules* **1996**, *29*, 3639.
(6) McLeish, T. C. B.; Allgaier, J.; Bick, D. K.; Bishko, G.; Biswas, P.; Blackwell, R.; Blottiere, B.; Clarke, N.; Gibbs, B.; Groves, D. J.; Hakiki, A.; Heenan, R. K.; Johnson, J. M.; Kant, R.; Read, D. J.; Young, R. N. *Macromolecules* **1999**, *32*, 6734.
(7) Daniels, D. R.; McLeish, T. C. B.; Kant, R.; Crosby, B. J.; Young, R. N.; Pryke, A.; Allgaier, J.; Groves, D. J.; Hawkins, R. J. *Rheol. Acta* **2001**, *40*, 403.
(8) Perny, S.; Allgaier, J.; Cho, D.; Lee, W.; Chang, T. *Macromolecules* **2001**, *34*, 5408.
(9) Chang, T. *J. Polym. Sci., Polym. Phys. Ed.* **2005**, *43*, 1591.
(10) Li, S. W.; Park, H. E.; Dealy, J. M.; Maric, M.; Lee, H.; Im, K.; Choi, H.; Chang, T.; Rahman, M. S.; Mays, J. *Macromolecules* **2011**, *44*, 208.
(11) Chambon, P.; Fernyhough, C. M.; Im, K.; Chang, T.; Das, C.; Embery, J.; McLeish, T. C. B.; Read, D. J. *Macromolecules* **2008**, *41*, 5869.
(12) Wang, Z. W.; Chen, X.; Larson, R. G. *J. Rheol.* **2010**, *54*, 223.
(13) Das, C.; Inkson, N. J.; Read, D. J.; Kelmanson, M. A. *J. Rheol.* **2006**, *50*, 207.
(14) Rahman, M. S.; Aggarwal, R.; Larson, R. G.; Dealy, J. M.; Mays, J. *Macromolecules* **2008**, *41*, 8225.
(15) Ryu, J.; Chang, T. *Anal. Chem.* **2005**, *77*, 6347.
(16) Park, S. J.; Larson, R. G. *J. Rheol.* **2005**, *50*, 21.
(17) Park, S. J.; Shanbhag, S.; Larson, R. G. *Rheol. Acta* **2005**, *44*, 319–330.
(18) Chen, X.; Costeux, C.; Larson, R. G. *J. Rheol.* **2010**, *54*, 1185.
(19) Chen, X.; Stadler, F. J.; Munstedt, H.; Larson, R. G. *J. Rheol.* **2010**, *54*, 393.
(20) Larson, R. G. *Macromolecules* **2001**, *34*, 4556.
(21) McLeish, T. C. B. *Eur. Phys. Lett.* **1988**, *6*, 511.
(22) Roovers, J. *Macromolecules* **1984**, *17*, 1196.
(23) Lee, H. C.; Chang, T.; Harville, S.; Mays, J. W. *Macromolecules* **1998**, *31*, 690.
(24) Synder, L. R.; Kirkland, J. J. *Introduction to Modern Liquid Chromatography*, 2nd ed.; Wiley-Interscience: New York, 1979.
(25) Lee, W.; Lee, H.; Cha, J.; Chang, T.; Hanley, K. J.; Lodge, T.P. *Macromolecules* **2000**, *33*, 5111.
(26) Ryu, J.; Im, K.; Yu, W.; Park, J.; Chang, T.; Lee, K.; Choi, N. *Macromolecules* **2004**, *37*, 8805.
(27) Li, S. W. Rheology of Branched Polybutadiene – Modeling Polydispersity. Doctoral Dissertation, University of McGill, 2010.
(28) Daniels, D. R.; McLeish, T. C. B.; Crosby, B. J.; Young, R. N.; Fernyhough, C. M. *Macromolecules* **2001**, *34*, 7025.
(29) Inkson, N. J.; Graham, R. S.; McLeish, T. C. B.; Groves, D. J.; Fernyhough, C. M. *Macromolecules* **2006**, *39*, 4217.